

Second-Harmonic Generation within the $P2_12_12_1$ Space Group, in a Series of Chiral (Salicylaldiminato)tin Schiff Base Complexes

José María Rivera, Horacio Reyes, Armando Cortés, and Rosa Santillan

Departamento de Química, Centro de Investigación y Estudios Avanzados del IPN, Apdo. Postal 14-740, 07000 México D. F.

Pascal G. Lacroix* and Christine Lepetit

Laboratoire de Chimie de Coordination du CNRS, 205 route de Narbonne, 31077 Toulouse, France

Keitaro Nakatani

PPSM, Ecole Normale Supérieure de Cachan, UMR 8531, 61 Avenue du Pdt Wilson, 94235 Cachan, France

Norberto Farfán*

Departamento de Química Orgánica, Facultad de Química, Universidad Nacional Autónoma de México, Ciudad Universitaria, 04510, México, D. F., México

Received July 20, 2005. Revised Manuscript Received December 16, 2005

A series of 10 (**2–11**) new chiral (salicylaldiminato)tin Schiff base complexes obtained from the Schiff base condensation of 4-(diethylamino)salicylaldehyde and various amino acids, in the presence of diphenyltin oxide, is reported together with the parent achiral (**1**) derivative. Compounds **2–7** crystallize in the $P2_12_12_1$ orthorhombic space group, and their quadratic nonlinear optical properties are investigated. At the molecular level, the derivatives possess similar electronic spectra ($\lambda_{\text{max}} \approx 395$ nm), and hence molecular hyperpolarizabilities (β), in relation to the same π -conjugated “push–pull” electronic structure. In the solid state, they exhibit efficiencies in second-harmonic generation (SHG) up to 8 times that of urea. The SHG intensities of chromophores **2–6** appear largely correlated with a simple “degree of chirality” (d_χ) parameter, defined from the molecular geometries. The intriguing issue of a possible quantification of chirality by means of SHG measurement is addressed.

Introduction

Metal complexes exhibiting quadratic nonlinear optical (NLO) properties have actively been investigated over the past decade.^{1–3} Among them, the most promising classes are (i) the push–pull metal porphyrin derivatives, which exhibit very large molecular hyperpolarizabilities,⁴ (ii) the bipyridyl–metal complexes, which provide a route toward nontraditional octupolar geometries,^{2a,5} (iii) the push–pull ruthenium pyridine derivatives, which have recently appeared as convincing redox-based molecular switches,⁶ and the salicylaldiminato metal Schiff base complexes,³ which have

provided nontraditional NLO chromophores, in which additional (e.g., ferromagnetic coupling,⁷ or spin transition phenomenon⁸) properties could lead to molecular materials with enhanced electronic capabilities.

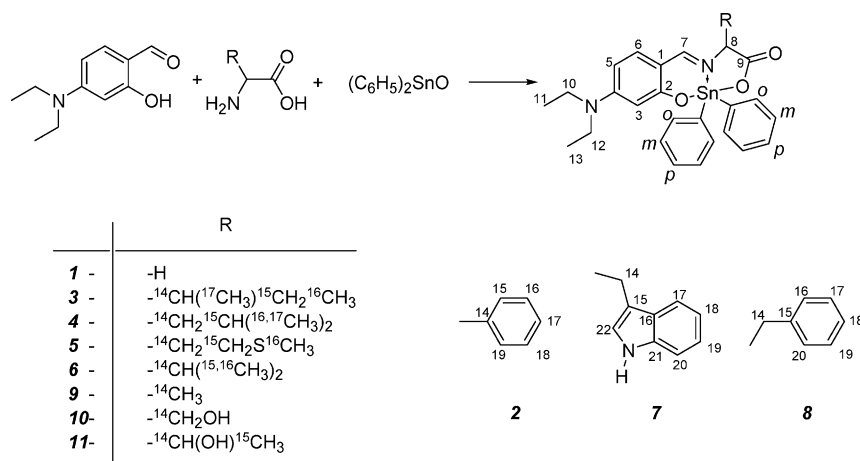
In molecular materials the solid-state NLO response is quantified by $\chi^{(2)}$ (quadratic susceptibility), which is ultimately related to (i) the underlying molecular hyperpolarizability (β) and (ii) to structural parameters, expressing the necessary condition for solid-state noncentrosymmetry.⁹ While the search for chromophores with enhanced β value has efficiently been boosted by the capabilities of organic synthesis,¹⁰ in concert with computational quantum procedures,¹¹ the engineering of chromophores into noncentrosymmetric crystal environments is empirical, with the outcome of many solid-state engineering strategies frequently being uncertain. As is well-known, it is not possible to predict crystal geometries from molecular geometries.¹² Neverthe-

* To whom correspondence should be addressed. E-mail: Pascal@lcc-toulouse.fr (P.G.L.); norberto.farfán@gmail.com (N.F.).

- (1) Coe, B. J. In *Comprehensive Coordination Chemistry II*; McCleverty J. A., Meyer, T. J., Eds.; Elsevier Pergamon: Oxford, U.K., 2004; Vol. 9, pp 621–687.
- (2) (a) Le Bozec, H.; Renouard, T. *Eur. J. Inorg. Chem.* **2000**, 229. (b) Whittall, I. R.; McDonagh, A. M.; Humphrey, M. G.; Samoc, M. *Adv. Organomet. Chem.* **1998**, 42, 291. (c) Verbiest, T.; Houbrechts, S.; Kauranen, M.; Clays, K.; Persoons, A. *J. Mater. Chem.* **1997**, 7, 2175. (d) Long, N. J. *Angew. Chem. Int. Ed. Engl.* **1995**, 34, 21.
- (3) (a) Di Bella, S. *Chem. Soc. Rev.* **2001**, 30, 355. (b) Lacroix, P. G. *Eur. J. Inorg. Chem.* **2001**, 339.
- (4) Le Cours, S. M.; Guan, H. W.; Dio Magno, S. G.; Wang, C. H.; Therien, M. J. *J. Am. Chem. Soc.* **1996**, 118, 1497.
- (5) Maury, O.; Le Bozec, H. *Acc. Chem. Res.* **2005**, 38, 691.
- (6) (a) Coe, B. J. *Chem. Eur. J.* **1999**, 5, 2464. (b) Coe, B. J.; Houbrechts, S.; Asselberghs, I.; Persoons, A. *Angew. Chem., Int. Ed.* **1999**, 38, 366.

- (7) Margeat, O.; Lacroix, P. G.; Costes, J. P.; Donnadieu, B.; Lepetit, C.; Nakatani, K. *Inorg. Chem.* **2004**, 43, 4743.
- (8) Averseng, F.; Lepetit, C.; Lacroix, P. G.; Tuchagues, J. P. *Chem. Mater.* **2000**, 12, 2225.
- (9) Williams, D. J. *Angew. Chem., Int. Ed. Engl.* **1984**, 23, 690.
- (10) (a) *Nonlinear Optical Properties of Organic Molecules and Crystals*; Chemla, D. S., Zyss, J., Eds.; Academic Press: New York, 1987. (b) *Molecular Nonlinear Optics*; Zyss, J., Ed.; Academic Press: New York, 1994.
- (11) Kanis, D. R.; Ratner, M. A.; Marks, T. J. *Chem. Rev.* **1994**, 94, 195.

Scheme 1



less, chirality has emerged since the birth of molecular nonlinear optics as the only crystal-engineering strategy, which guaranties that crystallization of a pure enantiomer will necessarily occur in a noncentrosymmetric space group.¹³

Along this line, the present contribution reports on the syntheses of a series of 10 (**2–11**) chiral (4-diethylaminosalicylaldiminato)tin chromophores, derived from a parent achiral molecule (**1**), reported as a reference (Scheme 1). In a research effort aimed at finding a structure–property relationship in these derivatives, we focus our investigations on the six compounds (**2–7**), which crystallize in the same noncentrosymmetric $P2_12_1$ space group, and on the nonchiral reference (**1**). These chromophores are based on the same π -conjugated electronic skeleton, and therefore, their electronic spectra will be found roughly similar, leading to the assumption that their molecular NLO response (β) is the same in any case. Their different solid-state NLO properties will be tentatively discussed in relation with a molecular “degree of chirality” calculated with the structural parameters available.

Experimental Section

Starting Materials and Equipment. All starting materials were purchased from Aldrich Chemical Co. and used without further purification. Melting points were obtained on a Gallenkamp MFB-595 apparatus and are uncorrected. Infrared spectra were measured on a Perkin-Elmer 16F-PC FT-IR spectrometer. ¹H, ¹¹⁹Sn, and ¹³C NMR spectra were recorded on Bruker Avance DPX 300 and JEOL Eclipse + 400 spectrometers. Chemical shifts (ppm) are relative to (CH₃)₄Si for ¹H and ¹³C and to Sn(CH₃)₄, for ¹¹⁹Sn. Mass spectra were recorded on a HP 5989A spectrometer. UV–vis spectra were recorded on a Perkin-Elmer Lambda 12 UV spectrophotometer and optical rotations on a Perkin-Elmer 241 polarimeter. Elemental analyses were carried out on a Thermo Finnigan Flash 1112 elemental analyzer.

Syntheses. Compounds **1–11** were synthesized by refluxing 4-diethylaminosalicylaldehyde (1 equiv), diphenyltin oxide (1 equiv), and the corresponding amino acid (1 equiv) in acetonitrile for 36 h, using a Dean–Stark trap.

2,2-Diphenyl-(4'-diethylaminobenzo[h])-6-aza-1,3-dioxo-6-en-2-stannacyclononen-4-one 1. ¹H NMR (300.13 MHz, CDCl₃) [δ , ppm]: 1.28 (6H, t, J = 7.0 Hz, H-11, H-13), 3.46 (4H, q, J = 7.0 Hz, H-10, H-12), 4.17 and 4.20 (2H, AB, J = 12.6 Hz, H-8a, H-8b), 6.16 (1H, dd, J = 2.4 Hz, J = 9.0 Hz, H-5), 6.24 (1H, d, J = 2.4 Hz, H-3), 6.87 (1H, d, J = 9.0 Hz, H-6), 7.37–7.49 (6H, m, H-*meta*, H-*para*), 7.87 (1H, s, H-7), 7.92–7.98 (4H, m, H-*ortho*). ¹³C NMR (75.47 MHz, CDCl₃) [δ , ppm]: 12.91 (C11, C13), 44.98 (C10, C12), 56.21 (C-8), 100.59 (C3), 105.06 (C5), 108.59 (C1), 128.87 (C-*meta*), 130.55 (C-*para*), 136.69 (C-*ortho*), 137.76 (C6), 138.87 (C-*ipso*), 155.72 (C4), 167.65 (C7), 170.96 (C2), 171.95 (C9). ¹¹⁹Sn NMR (111.88 MHz, CDCl₃) [δ , ppm]: –332.9.

2,2,5-Triphenyl-(4'-diethylaminobenzo[h])-6-aza-1,3-dioxo-6-en-2-stannacyclononen-4-one 2. ¹H NMR (300.13 MHz, CDCl₃) [δ , ppm]: 1.26 (6H, t, J = 7.0 Hz, H-11, H-13), 3.46 (4H, q, J = 7.0 Hz, H-10, H-12), 5.09 (1H, s, H-8), 6.15 (1H, dd, J = 2.2 Hz, J = 9.2 Hz, H-5), 6.23 (1H, d, J = 2.2 Hz, H-3), 6.80 (1H, d, J = 9.2 Hz, H-6), 7.19–7.23 (5H, m, H-15–H-19), 7.41–7.48 (6H, m, H-*meta*, H-*para*), 7.80 (1H, s, H-7), 7.94–7.99 (4H, m, H-*ortho*). ¹³C NMR (75.47 MHz, CDCl₃) [δ , ppm]: 13.23 (C11, C13), 45.35 (C10, C12), 70.40 (C8), 100.88 (C3), 105.46 (C-5), 109.35 (C-1), 128.17 (C16, C-18), 128.53 (C17), 129.20 and 129.25 (C-*meta*), 129.37 (C15, C19), 130.84 and 130.88 (C-*para*), 137.06 and 137.11 (C-*ortho*), 138.42 (C6), 139.16 and 139.42 (C-*ipso*) 139.86 (C14), 156.23 (C4), 169.10 (C7), 171.41 (C2), 173.31 (C9). ¹¹⁹Sn NMR (111.88 MHz, CDCl₃) [δ , ppm]: –337.6.

2,2-Diphenyl-5-((1-methyl)propyl)-(4'-diethylaminobenzo[h])-6-aza-1,3-dioxo-6-en-2-stannacyclononen-4-one 3. ¹H NMR (400 MHz, CDCl₃) [δ , ppm]: 0.80 (3H, t, J = 7.3 Hz, H-16), 0.85 (3H, d, J = 7.0 Hz, H-17), 1.11–1.21 (1H, m, H-15a), 1.25 (6H, t, J = 7.0 Hz, H-11, H-13), 1.54–1.60 (1H, m, H-15b), 1.82–1.92 (1H, m, H-14), 3.45 (4H, q, J = 7.0 Hz, H-10, H-12), 3.93 (1H, d, J = 3.6 Hz, H-8), 6.19 (1H, dd, J = 2.6 Hz, J = 9.0 Hz, H-5), 6.25 (1H, d, J = 2.6 Hz, H-3), 6.93 (1H, d, J = 9.0 Hz, H-6), 7.30–7.49 (6H, m, H-*meta*, H-*para*), 7.80–7.82 (2H, m, H-*ortho*), 7.86 (1H, s, H-7), 8.01–8.08 (2H, m, H-*ortho*). ¹³C NMR (100.5 MHz, CDCl₃) [δ , ppm]: 12.00 (C16), 12.89 (C11, C13), 15.35 (C17), 25.75 (C15), 42.58 (C14), 44.98 (C10, C12), 72.01 (C8), 100.85 (C-3), 104.97 (C-5), 108.68 (C-1), 129.69 and 128.73 (C-*meta*), 130.26 (C-*para*), 130.37 (C-*para*), 136.66 and 136.74 (C-*ortho*), 137.79 (C6), 138.77 and 139.23 (C-*ipso*), 155.51 (C4), 171.06 (C2), 167.79 (C7), 173.87 (C9). ¹¹⁹Sn NMR (111.88 MHz, CDCl₃) [δ , ppm]: –337.4.

2,2-Diphenyl-5-((2-methyl)propyl)-(4'-diethylaminobenzo[h])-6-aza-1,3-dioxo-6-en-2-stannacyclononen-4-one 4. ¹H NMR (400 MHz, CDCl₃) [δ , ppm]: 0.79 (3H, d, J = 6.2 Hz, H-16), 0.87 (3H,

(12) (a) Gavezzotti, A. *Acc. Chem. Res.* **1994**, 27, 309. (b) Hulliger, J.; Bebie, H.; Kluge, S.; Quintel, A. *Chem. Mater.* **2002**, 14, 1523.

(13) For an early and deeply studied example, see: Oudar, J.; Hierle, R. J. *Appl. Phys.* **1977**, 48, 2669.

d, $J = 6.2$ Hz, H-17), 1.25 (6H, t, $J = 7.0$ Hz, H-11, H-13), 1.47–1.51 (1H, m, H-15), 1.66–1.77 (2H, m, H-14), 3.45 (4H, q, $J = 7.0$ Hz, H-10, H-12), 4.03 (1H, dd, $J = 5.1$, 8.4 Hz H-8), 6.19 (1H, dd, $J = 2.6$ Hz, $J = 9.0$ Hz, H-5), 6.24 (1H, d, $J = 2.6$ Hz, H-3), 6.93 (1H, d, $J = 9.0$ Hz, H-6), 7.35–7.43 (6H, m, H-*meta*, H-*para*), 7.82 (1H, s, H-7), 7.85–7.87 and 7.97–7.99 (2H each, m, H-*ortho*). ^{13}C NMR (100.5 MHz, CDCl_3) [δ , ppm]: 12.88 (C11, C13), 22.17 and 23.08 (C16, C17), 23.09 (C15), 44.98 (C10, C12), 45.96 (C14), 66.49 (C8), 100.91 (C-3), 104.91 (C-5), 108.53 (C-1), 128.77 and 128.85 (C-*meta*), 130.38 and 130.52 (C-*para*), 136.46 and 136.85 (C-*ortho*), 137.65 (C6), 138.66 (C-*ipso*), 138.93 (C-*ipso*), 155.48 (C4), 167.03 (C7), 170.89 (C2), 175.12 (C9). ^{119}Sn NMR (111.88 MHz, CDCl_3) [δ , ppm]: –339.5.

2,2-Diphenyl-5-(1-methylsufanyl)-(4'-diethylaminobenzo[h])-6-aza-1,3-dioxo-6-en-2-stannacyclononen-4-one 5. ^1H NMR (300.13 MHz, CDCl_3) [δ , ppm]: 1.27 (6H, t, $J = 7.0$ Hz, H-11, H-13), 1.89 (3H, s, H-16), 2.01–2.07 (1H, m, H-15a), 2.10–2.17 (1H, m, H-15b), 2.30–2.37 (1H, m, H-14a), 2.45–2.49 (1H, m, H-14b), 3.47 (4H, q, $J = 7.0$ Hz, H-10, H-12), 4.23 (1H, t, $J = 5.7$ Hz, H-8), 6.21 (1H, dd, $J = 2.2$ Hz, $J = 9.2$ Hz, H-5), 6.24 (1H, d, $J = 2.2$ Hz, H-3), 6.94 (1H, d, $J = 9.2$ Hz, H-6), 7.34–7.45 (3H, m, H-*meta*, H-*para*), 7.83–7.86 (2H, m, H-*ortho*), 7.95–7.98 (3H, m, H-7, H-*ortho*). ^{13}C NMR (75.47 MHz, CDCl_3) [δ , ppm]: 13.22 (C11, C13), 15.60 (C16), 29.80 (C14), 35.37 (C-15), 45.34 (C10, C12), 66.05 (C8), 101.07 (C3), 105.45 (C-5), 109.03 (C-1), 129.14 and 129.24 (C-*meta*), 130.77 and 130.91 (C-*para*), 136.85 and 137.08 (C-*ortho*), 138.18 (C6), 138.90 and 139.24 (C-*ipso*), 156.02 (C4), 167.88 (C7), 171.32 (C2), 174.76 (C9). ^{119}Sn NMR (111.88 MHz, CDCl_3) [δ , ppm]: –338.7.

2,2-Diphenyl-5-((1-methyl)ethyl)-(4'-diethylaminobenzo[h])-6-aza-1,3-dioxo-6-en-2-stannacyclononen-4-one 6. ^1H NMR (400 MHz, CDCl_3) [δ , ppm]: 0.83 (3H, d, $J = 6.6$ Hz, H-15), 0.93 (3H, d, $J = 6.6$ Hz, H-16), 1.27 (6H, t, $J = 7.0$ Hz, H-11, H-13), 2.22–2.31 (1H, m, H-14), 3.46 (4H, q, $J = 7.0$ Hz, H-10, H-12), 3.84 (1H, d, $J = 4.0$ Hz, H-8), 6.20 (1H, dd, $J = 2.2$, 9.6 Hz, H-5), 6.25 (1H, d, $J = 2.2$ Hz, H-3), 6.93 (1H, d, $J = 9.6$ Hz, H-6), 7.33–7.43 (6H, m, H-*meta*, H-*para*), 7.78–7.81 (2H, m, H-*ortho*), 7.84 (1H, s, H-7), 8.01–8.04 (2H, m, H-*ortho*). ^{13}C NMR (100.5 MHz, CDCl_3) [δ , ppm]: 12.89 (C11, C13), 18.44 (C15), 19.19 (C-16), 34.94 (C-14), 44.99 (C10, C12), 73.08 (C8), 100.87 (C3), 105.01 (C5), 108.59 (C1), 128.74 (C-*meta*), 130.29 (C-*para*), 130.42 (C-*para*), 136.67 and 136.72 (C-*ortho*), 137.86 (C6), 138.67 (C-*ipso*), 139.13 (C-*ipso*), 155.51 (C4), 168.06 (C7), 171.33 (C2), 174.29 (C9). ^{119}Sn NMR (111.88 MHz, CDCl_3) [δ , ppm]: –336.4.

2,2-Diphenyl-5-(1H-indole-3-methyl)-(4'-diethylaminobenzo[h])-6-aza-1,3-dioxo-6-en-2-stannacyclononen-4-one 7. ^1H NMR (300.13 MHz, CDCl_3) [δ , ppm]: 1.26 (6H, t, $J = 7.1$ Hz, H-11, H-13), 2.90 (1H, dd, $J = 9.2$ Hz, $J = 14.0$ Hz, H-14a), 3.43 (4H, q, $J = 7.1$ Hz, H-10, H-12), 3.62 (1H, dd, $J = 3.2$ Hz, $J = 14.0$ Hz, H-14b), 4.22 (1H, dd, $J = 3.2$ Hz, $J = 9.2$ Hz, H-8), 6.03 (1H, dd, $J = 2.2$ Hz, $J = 9.1$ Hz, H-5), 6.20 (1H, d, $J = 2.2$ Hz, H-3), 6.37 (1H, d, $J = 9.1$ Hz, H-6), 6.66 (1H, d, $J = 2.2$ Hz, H-22), 6.91 (1H, s, H-7), 7.06 (1H, dd, $J = 0.7$ Hz, $J = 7.6$ Hz, H-18), 7.14 (1H, dt, $J = 1.0$ Hz, $J = 7.6$ Hz, H-19), 7.25 (1H, d, $J = 7.7$ Hz, H-20), 7.33–7.45 (6H, m, H-*meta*, H-*para*), 7.59 (1H, d, $J = 8.3$ Hz, H-17), 7.84–7.89 (4H, m, H-*ortho*), 8.24 (1H, br, NH). ^{13}C NMR (75.47 MHz, CDCl_3) [δ , ppm]: 13.21 (C11, C13), 32.73 (C14), 45.18 (C10, C12), 67.81 (C8), 100.94 (C3), 104.89 (C5), 108.48 and 109.69 (C1 and C15), 111.94 (C20), 119.18 (C17), 120.21 (C19), 122.62 (C18), 125.18 (C22), 127.17 (C16), 129.08 and 129.16 (C-*meta*), 130.54 and 130.67 (C-*para*), 136.66 and 137.07 (C-*ortho*), 136.71 (C-21) 137.89 (C6), 138.95 and 139.56 (C-*ipso*), 155.64 (C4), 167.76 (C7), 170.95 (C-2), 175.47 (C-9). ^{119}Sn NMR (111.88 MHz, CDCl_3) [δ , ppm]: –340.7.

2,2-Diphenyl-5-benzyl-(4'-diethylaminobenzo[h])-6-aza-1,3-dioxo-6-en-2-stannacyclononen-4-one 8. ^1H NMR (300.13 MHz, CDCl_3) [δ , ppm]: 1.25 (6H, t, $J = 7.0$ Hz, H-11, H-13), 2.78 (1H, dd, $J = 9.5$ Hz, $J = 13.6$ Hz, H-14a), 3.35–3.50 (5H, m, H-10, H-12, H-14b), 4.13 (1H, dd, $J = 3.3$ Hz, $J = 9.5$ Hz, H-8), 6.09 (1H, dd, $J = 2.3$ Hz, 9.0 Hz, H-5), 6.22 (1H, d, $J = 2.3$ Hz, H-3), 6.51 (1H, d, $J = 9.0$ Hz, H-6), 6.91 (1H, s, H-7), 6.99–7.10 (5H, m, H-16–H-20), 7.35–7.42 (6H, m, H-*meta*, H-*para*), 7.84–7.88 and 7.92–7.95 (2H each, m, H-*ortho*). ^{13}C NMR (75.47 MHz, CDCl_3) [δ , ppm]: 13.22 (C11, C13), 42.43 (C14), 44.22 (C10, C12), 69.59 (C8), 100.95 (C3), 105.11 (C5), 108.51 (C1), 127.40 (C18), 129.09 (C17, C19, C-*meta*), 129.20 (C-*meta*), 130.53 (C-*ortho*, C16, C20), 130.70 and 130.76 (C-*para*), 136.06 (C15), 136.81 and 137.10 (C-*ortho*), 138.02 (C6), 138.74 and 139.47 (C-*ipso*), 155.84 (C4), 167.85 (C7), 171.17 (C2), 174.71 (C9). ^{119}Sn NMR (111.88 MHz, CDCl_3) [δ , ppm]: –339.7.

2,2-Diphenyl-5-methyl-(4'-diethylaminobenzo[h])-6-aza-1,3-dioxo-6-en-2-stannacyclononen-4-one 9. ^1H NMR (400 MHz, CDCl_3) [δ , ppm]: 1.25 (6H, t, $J = 7.0$ Hz, H-11, H-13), 1.46 (3H, d, $J = 7.5$ Hz, H-14), 3.45 (4H, q, $J = 7.0$ Hz, H-10, H-12), 4.08 (1H, q, $J = 7.5$, H-8), 6.16 (1H, dd, $J = 2.2$ Hz, 9.0 Hz, H-5), 6.22 (1H, d, $J = 2.2$ Hz, H-3), 6.91 (1H, d, $J = 9.0$ Hz, H-6), 7.32–7.47 (6H, m, H-*meta*, H-*para*), 7.84 (1H, s, H-7), 7.87–7.89 (2H, m, H-*ortho*), 7.96–7.98 (2H, m, H-*ortho*). ^{13}C NMR (100.5 MHz, CDCl_3) [δ , ppm]: 12.90 (C11, C13), 22.68 (C14), 44.98 (C10, C12), 62.69 (C8), 100.65 (C3), 104.94 (C5), 108.77 (C1), 128.80 and 128.89 (C-*meta*), 130.44 and 130.53 (C-*para*), 136.79 and 136.48 (C-*ortho*) 137.70 (C-6), 138.81 and 139.05 (C-*ipso*), 155.60 (C4), 167.04 (C7), 170.81 (C2), 175.44 (C9). ^{119}Sn NMR (111.88 MHz, CDCl_3) [δ , ppm]: –340.8.

2,2-Diphenyl-5-hydroxymethyl-(4'-diethylaminobenzo[h])-6-aza-1,3-dioxo-6-en-2-stannacyclononen-4-one 10. ^1H NMR (300.13 MHz, CDCl_3) [δ , ppm]: 1.27 (6H, t, $J = 7.0$ Hz, H-11, H-13), 3.46 (4H, q, $J = 7.0$ Hz, H-10, H-12), 3.65–3.78 (1H, m, H-8, H-14a), 3.89–3.99 (1H, s, H-14b), 4.10 (1H, t, $J = 5.6$ Hz, H-8), 6.17 (1H, d, $J = 8.9$, 2.2 Hz, H-5), 6.21 (1H, d, $J = 2.2$ Hz, H-3), 6.96 (1H, d, $J = 8.9$ Hz, H-6), 7.30–7.46 (6H, m, H-*meta*, H-*para*), 7.84–7.87 (2H, m, H-*ortho*), 7.92–7.95 (2H, m, H-*ortho*), 8.02 (1H, s, H-7). ^{13}C NMR (75.47 MHz, CDCl_3) [δ , ppm]: 13.20 (C11, C13), 45.31 (C10, C12), 66.03 (C14), 68.43 (C8), 100.98 (C3), 105.40 (C5), 109.11 (C1), 129.16 (C-*meta*), 129.21 and 130.78 (C-*para*), 130.85 (C-*para*), 136.79 and 137.01 (C-*ortho*), 138.49 (C6), 138.85 and 139.32 (C-*ipso*), 156.05 (C4), 168.81 (C7), 171.25 (C2), 174.11 (C9). ^{119}Sn NMR (111.88 MHz, CDCl_3) [δ , ppm]: –338.1.

2,2-Diphenyl-5-(1-hydroxyethyl)-(4'-diethylaminobenzo[h])-6-aza-1,3-dioxo-6-en-2-stannacyclononen-4-one 11. ^1H NMR (300.13 MHz, CDCl_3) [δ , ppm]: 1.01 (1H, d, $J = 5.4$ Hz, H-15), 1.28 (6H, t, $J = 7.1$ Hz, H-11, H-13), 3.48 (4H, q, $J = 7.1$ Hz, H-10, H-12), 3.92–3.98 (1H, m, H-14), 4.12 (1H, d, $J = 3.8$ Hz, H-8), 6.19 (1H, dd, $J = 2.3$ Hz, $J = 7.1$ Hz, H-5), 6.23 (1H, d, $J = 2.3$ Hz, H-3), 6.95 (1H, d, $J = 7.1$ Hz, H-6), 7.37–7.47 (6H, m, H-*meta*, H-*para*), 7.79–7.83 (2H, m, H-*ortho*), 7.90 (1H, s, H-7), 7.94–7.96 (2H, m, H-*ortho*). ^{13}C NMR (75.47 MHz, CDCl_3) [δ , ppm]: 13.21 (C11, C13), 18.95 (C15), 45.38 (C10, C12), 70.37 (C-8), 71.35 (C14), 100.96 (C3), 105.66 (C5), 109.14 (C1), 129.14 and 129.18 (C-*meta*), 130.80 and 130.87 (C-*para*), 136.92 and 136.96 (C-*ortho*), 138.40 (C6), 138.66 and 139.28 (C-*ipso*), 156.22 (C4), 168.53 (C7), 171.47 (C2), 174.60 (C9). ^{119}Sn NMR (111.88 MHz, CDCl_3) [δ , ppm]: –336.0.

Structure Analysis and Refinement. The single crystals suitable for X-ray structural studies were obtained by slow evaporation from a mixture of CH_2Cl_2 and hexane, for compounds 1–7. The crystal data were recorded on an Enraf Nonius-Fr590 Kappa-CCD ($\lambda_{\text{MoK}\alpha}$

Table 1. Crystallographic Data for Compounds 1–7

	1	2	3	4	5	6	7
Crystal Data							
chemical formula	C ₂₅ H ₂₆ N ₃ Sn	C ₃₁ H ₃₀ N ₂ O ₃ Sn	C ₂₉ H ₃₄ N ₂ O ₃ Sn	C ₂₉ H ₃₄ N ₂ O ₃ Sn	C ₂₈ H ₃₂ N ₂ O ₃ Sn	C ₂₈ H ₃₂ N ₂ O ₃ Sn	C ₃₄ H ₃₃ N ₃ O ₃ Sn·H ₂ O
mol wt	521.19	597.26	577.27	577.27	595.34	563.25	668.4
cryst size (mm)	0.2 × 0.2 × 0.1	0.1 × 0.2 × 0.1	0.2 × 0.1 × 0.1	0.2 × 0.1 × 0.1	0.1 × 0.2 × 0.1	0.2 × 0.1 × 0.1	0.2 × 0.2 × 0.1
cryst system	monoclinic	orthorhombic	orthorhombic	orthorhombic	orthorhombic	orthorhombic	orthorhombic
space group	<i>P</i> 2 ₁ / <i>c</i>	<i>P</i> 2 ₁ 2 ₁ 2 ₁	<i>P</i> 2 ₁ 2 ₁ 2 ₁	<i>P</i> 2 ₁ 2 ₁ 2 ₁	<i>P</i> 2 ₁ 2 ₁ 2 ₁	<i>P</i> 2 ₁ 2 ₁ 2 ₁	<i>P</i> 2 ₁ 2 ₁ 2 ₁
<i>a</i> (Å)	9.19670(10)	9.77550(10)	10.40930(10)	10.34540(10)	9.91760(10)	10.6965(2)	9.8608(3)
<i>b</i> (Å)	23.6789(5)	15.4529(2)	12.4258(2)	12.6901(2)	13.6235(2)	12.8584(2)	11.8409(5)
<i>c</i> (Å)	10.7839(2)	19.2506(3)	21.8373(5)	21.4191(4)	20.3957(4)	20.0495(3)	26.7634(12)
β (deg)	92.109(1)						
<i>V</i> (Å ³)	2346.79(7)	2907.99(7)	2824.52(8)	2811.99(7)	2755.71(7)	2757.61(8)	3125.0(7)
ρ_{calc} (Mg/m ³)	1.435	1.364	1.358	1.364	1.435	1.357	1.380
μ (Mo K α) (mm ⁻¹)	1.113	0.911	0.935	0.939	1.034	0.956	0.857
Data Collection							
radiation (Mo K α) (Å)	0.71073	0.71073	0.71073	0.71073	0.71073	0.71073	0.71073
scan mode	θ and ϕ	θ and ϕ	θ and ϕ	θ and ϕ	θ and ϕ	θ and ϕ	θ and ϕ
θ range (deg)	3.40–27.49	3.44–27.56	3.41–27.46	3.81–27.48	3.60–27.49	3.44–27.48	3.52–27.48
no. of rflns							
measured	9235	20467	6281	24085	21844	21809	4986
unique	9097	20424	6257	24034	21793	21755	4974
used	4115	5596	5249	5067	5205	4978	3879
Refinement							
refinement on	<i>F</i> ²	<i>F</i> ²	<i>F</i> ²	<i>F</i> ²	<i>F</i> ²	<i>F</i> ²	<i>F</i> ²
no. of variables	348	415	441	405	433	348	403
H atom treatment	obsd	obsd	obsd	obsd	obsd	obsd	calcd
<i>R</i> [<i>I</i> > 2 σ (<i>I</i>)] ^a	0.0311	0.0282	0.0305	0.0316	0.0313	0.0389	0.0418
<i>wR</i> ^b	0.0490	0.0415	0.0442	0.0504	0.0458	0.0578	0.0860
$\Delta\rho_{\text{max}}$ (e Å ⁻³)	0.512	0.295	0.337	0.371	0.631	0.536	0.338
$\Delta\rho_{\text{min}}$ (e Å ⁻³)	−0.380	−0.287	−0.316	−0.333	−0.674	−0.527	−0.337
GOF	1.016	1.035	1.028	1.020	1.029	1.026	1.040
Flack param		−0.04(1)	−0.05(2)	−0.03(2)	−0.06(2)	−0.04(3)	−0.04(3)

$$^a R = \sum(|F_o| - |F_c|)/\sum|F_o|. \quad ^b wR = [\sum w(|F_o| - |F_c|)^2/\sum wF_o^2]^{1/2}.$$

= 0.71073 Å, graphite monochromator, *T* = 293 K, CCD rotating images scan mode). The crystals were mounted on a Lindeman tube. Absorption corrections were performed within the SHELX-97¹⁴ program or by the semiempirical correction through MULTISCAN procedure (PLATON).¹⁵ All reflection data sets were corrected for Lorentz and polarization effects. The first structure solution was obtained using the SHELX-S-97 program and then SHELX-L-97 version 34 program¹⁴ was applied for refinement and output data. All software manipulations were done under the WIN-GX¹⁶ environment program set. Molecular perspectives were drawn under ORTEP 3¹⁷ drawing application. All heavier atoms were found by Fourier map difference and refined anisotropically. Some hydrogen atoms were found by Fourier maps differences and refined isotropically. The remaining hydrogen atoms were geometrically modeled and not refined. Crystal data for **1–7** are summarized in Table 1.

Tables of crystallographic parameters, atomic coordinates, anisotropic thermal parameters, bond distances, bond angles, as well as a listing of structure factors have been deposited with the Cambridge Crystallographic Data Centre (CCDC nos. 278483–278489 for compounds **1–7**, respectively). Copies of this information may be obtained free of charge from the director, CCDC, 12 Union Road, Cambridge, CB2 1EZ, U.K. (Fax: +44-1223-336-033. E-mail: deposit@ccdc.cam.ac.uk or <http://www.ccdc.cam.ac.uk>).

Theoretical Methods. The molecular hyperpolarizability was computed for the representative molecule **4** at the B3PW91/6-31+G*/LANL2DZ(Sn) level¹⁸ using the finite field (FF) proce-

dure included in the Gaussian98 package.¹⁹ The use of a pseudopotential allows the description of relativistic effects for Sn. The default value of field strength of 0.001 atomic units was used in the calculations. In this approach, β is obtained as the numerical partial derivative of the energy (*W*) with respect to the electric field (*E*), evaluated at zero field according to the following equation:

$$\beta_{ijk} = - \left(\frac{\partial^3 W}{\partial E_i \partial E_j \partial E_k} \right)_{E=0} \quad (1)$$

an expression which is only valid for the static field limit.¹¹ Following this approach, β is the magnitude of the vectorial hyperpolarizability ($\beta = \sqrt{(\beta_x)^2 + (\beta_y)^2 + (\beta_z)^2}$ with $\beta_i = \beta_{ixx} + \beta_{iyy} + \beta_{izz}$, after assumption of the Kleinman symmetry conditions.²⁰ The metrical parameters used for the calculation were taken from the present crystal structure. For the sake of simplification, dimethylamino groups (instead of diethylamino) were introduced in the calculations for compound **1** and **4**, by replacing the methyl group of the extremities by a hydrogen atom located at 0.95 Å.

Optical Measurements. The electronic spectra were recorded in chloroform, using a Perkin-Elmer Lambda 12 UV spectro-

(14) Sheldrick, G. M. *SHELX-97*; University of Göttingen: Göttingen, Germany, 1993.

(15) Spek, A. L. *J. Appl. Crystallogr.* **2003**, *36*, 7.

(16) Farrugia, L. J. *J. Appl. Crystallogr.* **1999**, *32*, 837.

(17) Farrugia, L. J. *J. Appl. Crystallogr.* **1997**, *30*, 565.

(18) (a) Becke, A. D. *J. Chem. Phys.* **1993**, *98*, 1372. (b) Perdew, J. P.; Wang, Y. *Phys. Rev. B* **1992**, *45*, 13244.

(19) Frisch, M. J.; Trucks, G. W.; Schlegel, H. B.; Scuseria, G. E.; Robb, M. A.; Cheeseman, J. R.; Zakrzewski, V. G.; Montgomery, J. A., Jr.; Stratmann, R. E.; Burant, J. C.; Dapprich, S.; Millam, J. M.; Daniels, A. D.; Kudin, K. N.; Strain, M. C.; Farkas, O.; Tomasi, J.; Barone, V.; Cossi, M.; Cammi, R.; Mennucci, B.; Pomelli, C.; Adamo, C.; Clifford, S.; Ochterski, J.; Petersson, G. A.; Ayala, P. Y.; Cui, Q.; Morokuma, K.; Malick, D. K.; Rabuck, A. D.; Raghavachari, K.; Foresman, J. B.; Cioslowski, J.; Ortiz, J. V.; Baboul, A. G.; Stefanov, B. B.; Liu, G.; Liashenko, A.; Piskorz, P.; Komaromi, I.; Gomperts, R.; Martin, R. L.; Fox, D. J.; Keith, T.; Al-Laham, M. A.; Peng, C. Y.; Nanayakkara, A.; Gonzalez, C.; Challacombe, M.; Gill, P. M. W.; Johnson, B.; Chen, W.; Wong, M. W.; Andres, J. L.; Gonzalez, C.; Head-Gordon, M.; Replogle, E. S.; Pople, J. A. *Gaussian 98*, revision A.7; Gaussian, Inc.: Pittsburgh, PA, 1998.

(20) Kleinman, D. A. *Phys. Rev.* **1962**, *126*, 1977.

photometer. The intensities were evaluated as the oscillator strengths, extracted from the spectra through the following relation:²¹

$$f = 4.315 \times 10^{-9} \int \epsilon \, d\nu \quad (2)$$

where the integration extends over the entire absorption band and ν is the wavenumber (cm^{-1}).

NLO Measurements. The measurements of second-harmonic generation (SHG) intensities in the solid state were carried out by the Kurtz–Perry powder test,²² using a nanosecond-pulsed Nd:YAG (10 Hz) laser. The fundamental radiation (1.064 μm) was used as the incident laser beam for SHG. The outcoming Stokes-shifted radiation at 1.907 μm generated by Raman effect in a hydrogen cell (1 m long, 50 atm) was used as an additional wavelength for SHG. The second-harmonic signal was detected by a photomultiplier and read on an ultrafast Tektronic TDS 620B oscilloscope. The samples were microcrystalline powders obtained by grinding and carefully calibrated in the 50–80 μm range. The powders were put between two glass plates (thickness of 0.2 mm).

Results and Discussion

Design and Characterization of Organotin (IV) Derivatives. An important class of diorganotin (IV) complexes are those derived from Schiff bases. Their investigation has initially been encouraged by the discovery of in vitro and in vivo antitumor activity in organotin(IV) derivatives.^{23–25} These types of compounds have also found application in homogeneous catalysis²⁶ and medicinal chemistry.²⁷

The syntheses of compounds **1–11** follow our general route toward push–pull Schiff bases built up from di-*n*-butyltin and diphenyltin oxide²⁸ or toward organotin derivatives containing various amino acid fragments.²⁹ They imply one-step condensations in acetonitrile, which require equimolecular quantities of 4-diethylaminosalicylaldehyde, diphenyltin oxide, and the corresponding amino acid. (Scheme 1).

The ^{13}C NMR spectra of **1–11** show the carbonyl signal between 170 and 171 ppm and the imine between 169 and 171 ppm, the corresponding iminic proton (H-7) appears between 7.80 and 8.01 ppm in the ^1H NMR spectra, with the exception of compounds **7** and **8**, where this signal is shifted to 6.91 ppm, due to the presence of the benzylic and indole substituents; this effect has been previously documented.²⁹ The ^{119}Sn NMR spectra for **1–11** show the tin signal in the range between –332 and –340 ppm, which is characteristic for these types of pentacoordinate tin derivatives containing nitrogen coordination.^{29–31} The infrared spectra for **1–11** show the band assigned to the imine bond at 1614 cm^{-1} , which is present in all compounds while the carbonyl stretching band appears between 1661 and 1681 cm^{-1} . Mass spectra do not show the molecular ion; the main fragment ion is $\text{M}^+ - \text{CH}_2\text{CO}$. The presence of the tin atom is easily detected due the isotopic abundances of tin.³² For the sake of simplification and homogeneity, the structure–NLO property relationship will be investigated in the next sections for the six derivatives which crystallize in the $P2_12_12_1$ space group (**2–7**), in relation to the nonchiral reference (**1**). The other four (**8–11**) chiral derivatives do not crystallize in the $P2_12_12_1$ space group and, therefore, cannot lead to reliable comparisons. Consequently, their properties are not reported in the present study.

Structure Description. The X-ray structures for compounds **1–7** evidence a pentacoordinated geometry around the tin atom (Figure 1), the oxygen atoms occupy axial positions. The N \rightarrow Sn distance are equal to 2.119(2), 2.114(2), 2.131(2), 2.121(3), 2.127(3), 2.123(3), and 2.125(3) Å for **1–7**, respectively, similar to those observed in other tin complexes.^{29–31} The Sn–O1 (phenol oxygen) bond length is shorter (2.069(3) to 2.081(2) Å) than the Sn–O2 (amino acid oxygen) bond (2.137(3) to 2.159(2) Å). The phenyl groups bonded to tin show very similar Sn–C bond lengths, in the 2.109(4) to 2.145(2) Å range.

The achiral complex **1** crystallizes in the centrosymmetric $P2_1/c$ monoclinic space group. A careful examination reveals that the 4-aminosalicylaldehyde fragment is roughly planar. More precisely, 15 atoms lie grossly in the same plane, namely, N1 and N2, C1–C8 (with their related hydrogen atoms H3, H5, H6, and H7), and O1. The largest deviation of 0.234(7) Å from this mean plane is observed at N2. This situation suggests that a π -electron delocalization takes place between the N2 donor atom and the imino (C7–N1) withdrawing group, leading to an intramolecular charge transfer, and hence to a potential NLO response. This possibility is illustrated in Scheme 2.

The six chiral compounds (**2–7**) crystallize in the non-centrosymmetric $P2_12_12_1$ orthorhombic space group. In the case of **2–6**, the asymmetric unit cell is built up from a single molecule. As observed in the parent chromophore **1**, a plane can be defined from the 15 atoms of the aminosalicylaldehyde

- (21) Orchin, M.; Jaffé, H. H. *Symmetry Orbitals, and Spectra*; John Wiley: New York, 1971; p 204.
- (22) (a) Kurtz, S. K.; Perry, T. T. *J. Appl. Phys.* **1968**, *39*, 3798. (b) Dougherty, J. P.; Kurtz, S. K. *J. Appl. Crystallogr.* **1976**, *9*, 145.
- (23) (a) Gielen, M.; Lelieveld, P.; de Vos, D.; Willem, R. In vitro antitumor activity of organotin compounds. In *Metal-Based Antitumor Drugs*; Gielen, M. F., Ed.; Freund Publishing House, London, 1998; Vol. 2, p 29. (b) Haiduc, I.; Silvestru, C. *Organometallics in Cancer Chemotherapy: Main Group Metal Compounds*; CRC Press: Boca Raton, FL, 1989; Vol. 1, p 129.
- (24) (a) Gielen, M. *Coord. Chem. Rev.* **1996**, *151*, 41. (b) Nath, M.; Pokharia, S.; Yadav, R. *Coord. Chem. Rev.* **2001**, *215*, 99.
- (25) (a) Gielen, M.; Willem, R. *Anticancer Res.* **1992**, *12*, 257. (b) Willem, R.; Bouhdid, A.; Biesemans, M.; Martins, J. C.; de Vos, D.; Tiekink, E. R. T.; Gielen, M. *J. Organomet. Chem.* **1996**, *514*, 203. (c) Nath, M.; Yadav, R.; Gielen, M.; Dalil, H.; de Vos, D.; Eng, G. *Appl. Organomet. Chem.* **1997**, *11*, 727. (d) de Vos, D.; Willem, R.; Gielen, M.; Wingerden, K. E.; Nooter, K. *Met.-Based Anti-tumour Drugs* **1998**, *5*, 179. (e) Mancilla, T.; Carrillo, L.; Zamudio-Rivera, L. S.; Camacho, C. C.; de Vos, D.; Kiss, R.; Darro, F.; Mahieu, B.; Tiekink, E. R. T.; Rahier, H.; Gielen, M.; Kemmer, M.; Biesemans, M.; Willem, R. *Appl. Organomet. Chem.* **2001**, *15*, 593.
- (26) (a) Orita, K.; Sakamoto, Y.; Hamada, K.; Mitsutome, A.; Otera, J. *Tetrahedron* **1999**, *55*, 2899. (b) Edelman, M. A.; Hitchcock, P. B.; Lappert, M. F. *J. Chem. Soc., Chem. Commun.* **1990**, 1116.
- (27) (a) Willem, R.; Bouhdid, A.; Biesemans, M.; Martins, J. C.; de Vos, D.; Tiekink, E. R. T.; Gielen, M. *J. Organomet. Chem.* **1996**, *514*, 203. (b) Gielen, M. *Coord. Chem. Rev.* **1996**, *151*, 41.
- (28) Reyes, H.; García, C.; Farfán, N.; Santillan, R.; Lacroix, P. G.; Lepetit, C.; Nakatani, K. *J. Organomet. Chem.* **2004**, *689*, 2303.
- (29) Beltran, H. I.; Zamudio-Rivera, L. S.; Mancilla, T.; Santillan, R.; Farfán, N. *Chem. Eur. J.* **2003**, *9*, 2291.

- (30) Smith, P. J.; Tupčiauskas, A. P. *Annual Reports on NMR Spectroscopy*, **1978**, *8*, 292.
- (31) Nath, M.; Yadav, R.; Gielen, M.; Dalil, H.; De Vos, D.; Eng, G. *Appl. Organomet. Chem.* **1997**, *2*, 727.
- (32) Lisow, M. R.; Spalding, T. R. *Mass Spectrometry of Inorganic and Organometallic Compounds*; Elsevier Scientific Publishing Company: Amsterdam-London-New York, 1973; p 209.

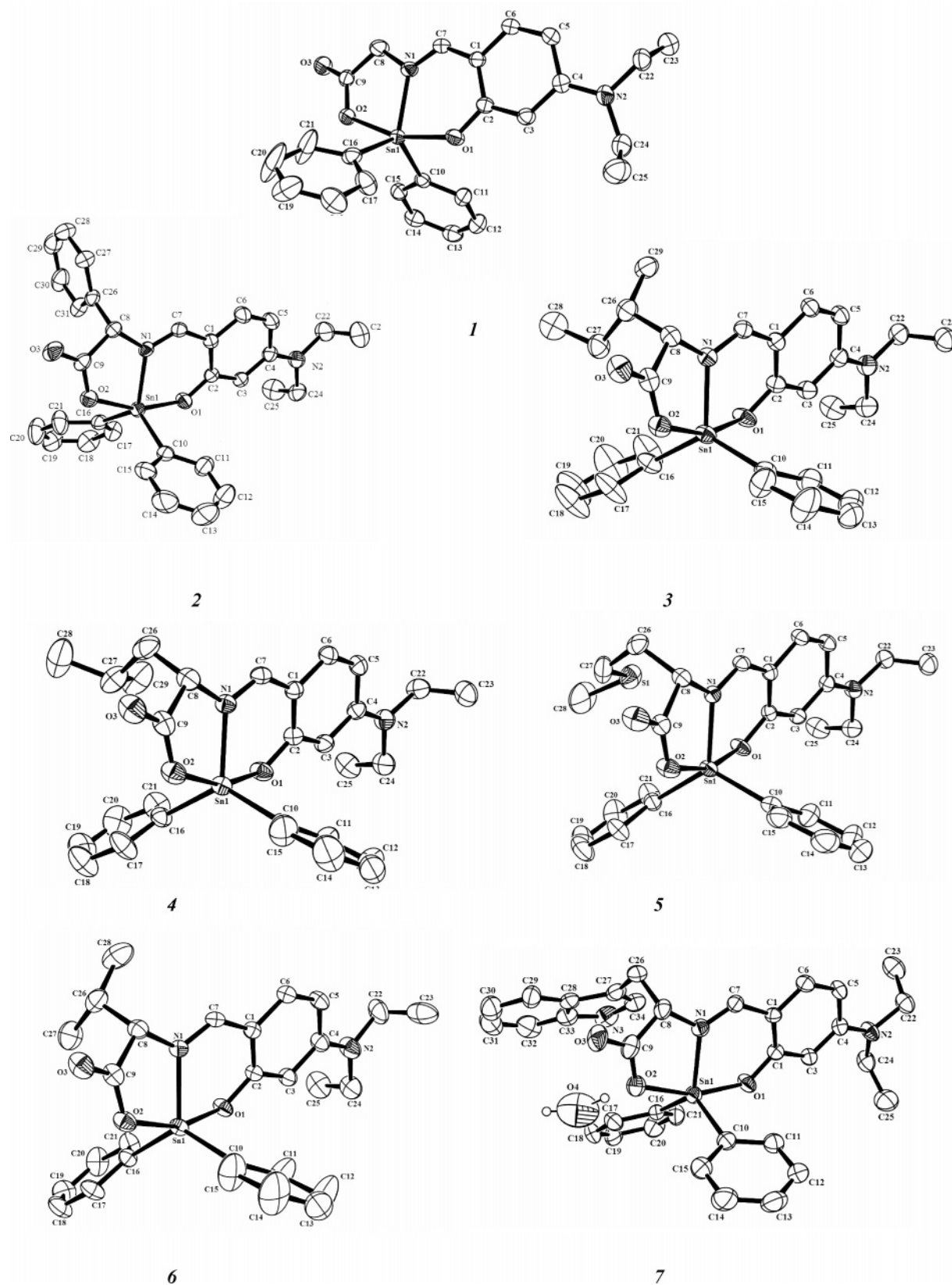


Figure 1. X-ray structures and atom labeling scheme for compounds **1**–**7**. Hydrogen atoms are omitted for clarity.

moieties, the main features of which are gathered in Table 2. In the solid state, the shortest intermolecular distances lie in the 2.4–2.6 Å range and correspond to weak intermolecular hydrogen bonds involving H atoms of imine or phenyl moieties and the lone pair of a carbonyl group. These

structural data are gathered in Table 3. In the case of compound **7**, a molecule of water is present in the asymmetric unit cell. This is illustrated in Figure 2. The water molecule acts as a bridge between two chromophores with two hydrogen bonds ($O3-H2 = 2.712$ Å and $O4-H4 =$

Scheme 2

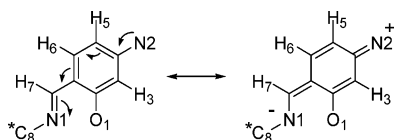


Table 2. Comparison of the Mean Planes Defined from Atoms N1 and N2, C1–C8, O1, H3, H5, H6, and H7 for Compounds 1–7, with Largest Deviation (Å) Observed from the Plane and Degree of Chirality (d_χ) Defined by Relation 3

compound	largest deviation observed from the mean plane		d_χ
	atom	distance	
1	N2	0.234	8×10^{-4}
2	C8	0.172	0.346
3	C8	−0.067	0.243
4	N1	0.077	0.266
5	N1	0.130	0.343
6	C6	0.073	0.157
7	N2	−0.137	0.686

Table 3. Shortest Intermolecular Distance (Å) in the Chiral Derivatives 2–7

compounds	shortest contact C=O...H–R	nature of H–R
2	2.36	H–C=N
3	2.55	H–C=N
4	2.57	phenyl
5	2.49	H–C=N
6	2.52	H–C=N
7	2.61	H–C=N

2.004 Å).³³ Therefore, and to a large extent, we can infer that, except for **7**, the differences in the molecular packings mostly reflect the differences of chromophore geometries.

In an attempt toward a possible quantification of the chirality of the tin complexes, a molecular “degree of chirality” (d_χ) defined from the substituents (e.g., $-\text{H}$ and $-\text{C}_6\text{H}_5$ for **2**) carried by the asymmetric atom C8 is tentatively introduced, from the crystal data available. In the present approach, d_χ is defined as follows:

$$d_\chi = \frac{\sum_i d_i m_i}{\text{MW}} \quad (3)$$

In this expression, d_i is the distance between atom i and the mean plane previously defined from the 15 atoms of the aminosalicylaldimine skeleton, m_i is the atomic mass of atom i , and MW is the total molecular weight of the chromophore, introduced in order to normalize the property. The summation runs over all the atoms of the substituents H and R (Scheme 1) linked to atom C8. Assuming this definition, the degree of chirality has the dimension of a distance and, therefore, quantifies “how far from being achiral the chromophore is”. More precisely, we can infer from eq 3 that two identical substituents on C8 (achiral molecule) lead to an almost vanishing d_χ value, while a bulky R substituent results in a “very chiral molecule” associated to a large d_χ . The **1–7** d_χ values are shown in Table 2.

Optical Spectra. The UV–vis spectra were recorded for compounds **1–7**, in chloroform. In any case, the spectra are

dominated by an intense transition located in the 390–400 nm range. A shoulder is present at higher energy. The UV–vis data are gathered in Table 4 for each **1–7** derivative. Except for **7**, where the oscillator strength is found reduced by about 10%, the table reveals that all the derivatives exhibit related spectra (energy and intensity). A representative spectrum has been deposited as Supporting Information in the case of **1**.

The knowledge of the origin of these intense transitions is not available from our DFT calculations. However, the frontier orbitals presented in Figure 3 suggest that a charge transfer may be expected from the amine group to the imine moiety. This observation is consistent with the previous report that the electronic spectra of this class of salicylaldiminato Schiff base complexes are dominated by $\pi-\pi^*$ transitions having charge-transfer character between the aminophenolate donor moieties and the imine acceptor group.^{7,34} This leads to sizable molecular NLO response (β), according to the following relation:³⁵

$$\beta_{2L} = \sum_i \frac{3e^2 \hbar f_i \Delta\mu_i}{2mE_i^3} \frac{E_i^4}{(E_i^2 - (2\hbar\omega)^2)(E_i^2 - (\hbar\omega)^2)} \quad (4)$$

in which, f_i , $\Delta\mu_i$, and E_i are the oscillator strength, the difference between ground and excited-state dipole moment, and the energy of the i th transition, respectively ($\hbar\omega$ being the energy of the incident laser beam). According to relation 4, “push–pull” molecules exhibiting similar UV–vis spectra should likely possess β values lying in the same range of magnitude. This assumption will be verified in the next section.

NLO Properties. The molecular hyperpolarizability calculated at the B3PW91/6-31G*/LANL2DZ(Sn) level on molecule **4**, on the basis of the present crystal structure, was found to be equal to $16.6 \times 10^{-30} \text{ cm}^5 \text{ esu}^{-1}$. The β orientation is shown in Figure 4. The origin of the charge transfer cannot be derived from the finite field (FF) procedure used in the present DFT calculation of the hyperpolarizability. Nevertheless, the available data can be compared to those obtained in a previous investigation conducted on a bis-(salicylaldiminato) nickel Schiff base derivative in which the same set of “push–pull” fragments were present.^{34a} Interestingly, Figure 4 shows that the charge-transfer direction within each salicylaldiminato unit of the previously reported nickel derivative is grossly that of the hyperpolarizability in the present tin complexes. This suggests that the properties are the same in both cases, therefore that the NLO response of the present tin derivatives is directly related to the salicylaldiminato fragment. More precisely, the angle between β and the mean plane previously defined from the 15 atoms of the 4-aminosalicylaldimine fragment is equal to 2.89° in **4**, in full agreement with the assumption that the NLO response arises from the salicylaldiminato framework, with-

(34) (a) Averseng, F.; Lacroix, P. G.; Malfant, I.; Dahan, F.; Nakatani, K. *J. Mater. Chem.* **2000**, *10*, 1013. (b) Averseng, F.; Lacroix, P. G.; Malfant, I.; Périssé, N.; Lepetit, C.; Nakatani, K. *Inorg. Chem.* **2001**, *40*, 3797.

(35) (a) Oudar, J. L. *J. Chem. Phys.* **1977**, *67*, 446. (b) Oudar, J. L.; Chemla, J. J. *J. Chem. Phys.* **1977**, *66*, 2664.

(33) Bondi, A. *J. Phys. Chem.* **1964**, *68*, 441.

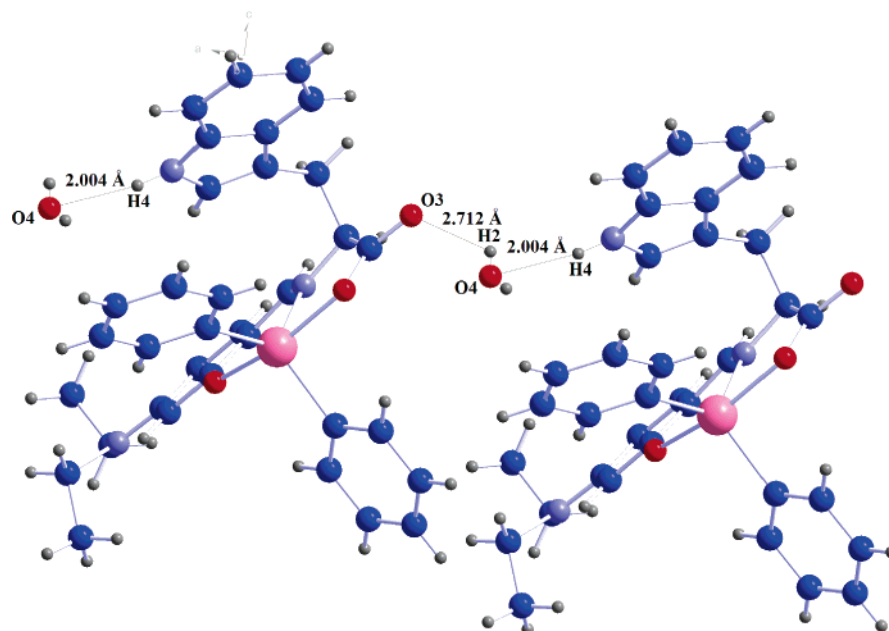


Figure 2. Intermolecular interactions in the cell of compound 7.

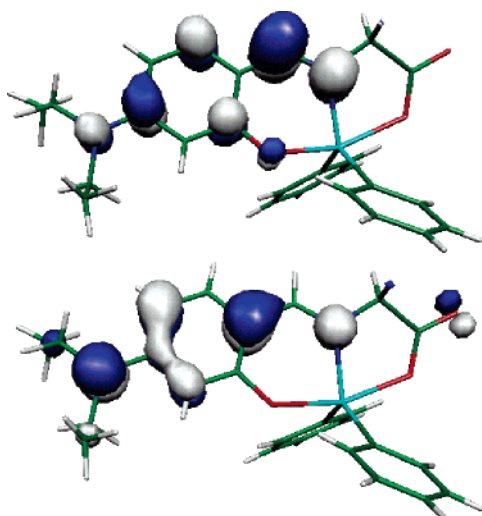


Figure 3. HOMO (bottom) and LUMO (top) frontier orbitals calculated at the B3PW91/6-31+G*/LANL2DZ(Sn) level for chromophore 4.

Table 4. Absorption Maxima (λ_{max} in nm) and Intensity (Extinction Coefficient ϵ in $\text{dm}^3 \text{mol}^{-1} \text{cm}^{-1}$ and Oscillator Strength f) of the Low-Energy Charge-Transfer Transition for the Tin Complexes

compounds	λ_{max}	ϵ	f
1	395	50 000	0.54
2	398	50 900	0.52
3	393	51 900	0.54
4	391	50 400	0.54
5	394	52 100	0.54
6	392	52 900	0.55
7	394	44 700	0.49

out any contribution of the chiral fragment. To further support this assumption, the β calculation has been performed on the achiral molecule **1**, in a conformation built up from the crystal structure of **4**. Doing so, the same π -conjugated electronic skeleton is present in both cases, and the differences in β reflect the effect of the chiral substituent, only. In these conditions, **1** exhibits a β value of $15.1 \times 10^{-30} \text{ cm}^5 \text{esu}^{-1}$, therefore very similar to that of **4**, while the angle between both hyperpolarizabilities is equal to 5.1° . This indicates that the magnitude and the direction of β are only

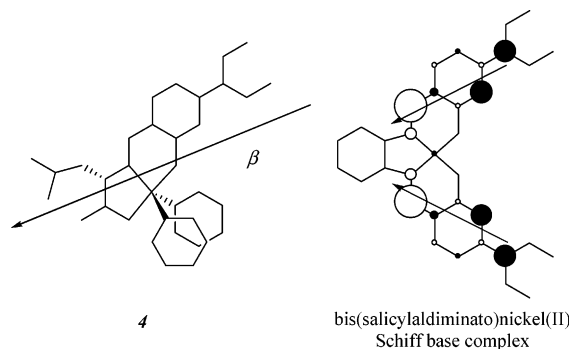


Figure 4. β orientation of chromophore **4**, compared with the charge-transfer axis of a related bis(salicylaldiminato)nickel(II) Schiff base complex (ref 34a), for which ZINDO data are available. On the nickel complex, the white (black) contribution is indicative of an increase (decrease) of electron density in the charge-transfer process.

slightly affected by the presence of an alkyl substituent on the asymmetric C8 atom in complexes **2–6**. By contrast, the presence of a π -conjugation on the chiral substituent of complex **7** may modify the overall charge-transfer behavior and lead to a significant difference in terms of hyperpolarizability. Finally, the spectroscopic and computational investigations lead to the conclusion that the tin derivatives **1–6** exhibit the same optical spectra, and hence NLO response at the molecular level, whatever the nature of the chiral alkyl substituent.

The SHG efficiencies measured by the Kurtz–Perry powder test are gathered in Table 5 at 1.064 and 1.907 μm . Although the derivatives are transparent in solution at the second-harmonic wavelength of 532 nm, the powdered samples may be slightly absorbent. More precisely, the powdered samples **2** and **7** are orange, and their SHG efficiency is reduced at the 1.064 μm incident wavelength. This effect is more important for **2**. Therefore, the comparison of the intrinsic SHG intensities has to be conducted at the 1.907 μm incident wavelength; all the samples exhibiting a perfect transparency at 953 nm. The first observation of the data gathered in Table 5 indicates that although the

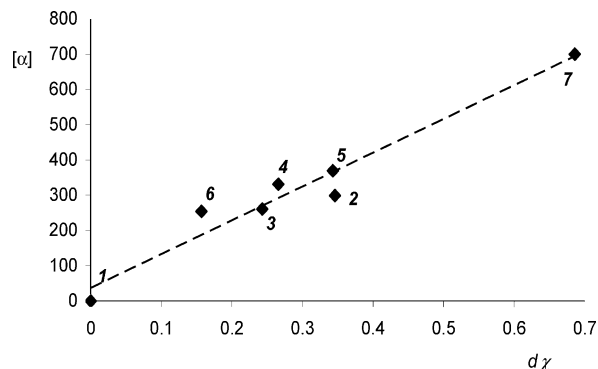
Table 5. Solid-State Powder Efficiencies at Various Laser Wavelengths (Referred to Urea) for Chromophores 2–7

compound	laser wavelength		d_{χ}
	1.064 μm	1.907 μm	
urea	1	1	
2	0.8	8.0	0.346
3	6.5	6.4	0.243
4	8.7	5.5	0.266
5	8.0	6.8	0.343
6	5.0	5.0	0.157
7	0.7	1.8	0.686

“push–pull” character and the length of the conjugated pathway are rather modest for 2–7, the SHG efficiencies are sizable and reach 8 times that of urea, in the best cases. As the β values are grossly similar in the series, the SHG intensities arise from different crystal packing, in relation with the different nature of the chiral substituents. All together these considerations lead to the intriguing issue of a possible quantification of chirality by means of NLO measurements. This will be evaluated in the last section.

An Attempt to Correlate the SHG Efficiencies with the Molecular Chirality. Lord Kelvin’s universally accepted definition relates the concept of chirality to that of reflection symmetry.³⁶ A molecule having such symmetry can be said to possess a “degree of chirality”³⁷ equal to zero, while a molecule without reflection symmetry can have a nonzero degree of chirality. Along this line, the intriguing issue of “how to quantify chirality” becomes naturally addressed. In an important paper, Mislow has reviewed various methods aimed at quantifying how far an object is from being achiral.³⁸ They also proposed a unification of chirality measurements.³⁹ Furthermore, Avnir and co-workers developed a continuous chirality measure (CCM) methodology to evaluate the distance of a chiral molecule to the nearest achiral parent.⁴⁰ All these approaches are computational investigations based on molecular geometrical features and would certainly benefit from comparisons with experimental measurements. However, chirality is not a physical observable, and direct measurements are not available. On the other hand, correlations have previously been observed between chirality and chemical behaviors, such as the enantioselective catalytic activity.⁴¹ As far as physical properties are involved, two different levels of investigation must be distinguished: (i) the molecular level and (ii) the solid-state level.

(i) At the molecular level, the degree of chirality (d_{χ}) as defined by relation 3, is compared with the specific rotation in Figure 5, in relation to the well-known use of optical activity to distinguish between chiral and achiral molecules. A correlation clearly appears on the figure, supported by the idea that, in a series of compounds having roughly the same

**Figure 5.** Specific rotations for compounds 2–7 expressed as a function of the degree of chirality d_{χ} .

chemical nature and π -electronic push–pull character, the more chiral molecules should exhibit the largest specific rotations. With this respect, the agreement appears satisfactory and leads to the relevance of our simple d_{χ} parameter to account for the molecular chirality in this series of tin complexes.

(ii) At the solid-state level, chiral molecules lead to noncentrosymmetric crystals and, hence, NLO active materials. The fact that a crystal is noncentrosymmetric does not guarantee that the molecular packing will be optimized for NLO effects. Therefore, it seems natural to think that the more chiral molecules may provide the more noncentrosymmetric crystals, which therefore may lead to the more efficient NLO materials. However, before any search for correlations between crystal SHG efficiencies and molecular degrees of chirality, several important issues must necessarily be addressed, especially those concerning the relationships between molecular structure and crystal structure. More precisely, the following requirements must be fulfilled. Requirement 1: as the SHG signal depends on the molecular hyperpolarizability, all the chromophores must exhibit the same β value (magnitude and direction). Requirement 2: as the macroscopic NLO properties arise from the orientation of the molecules in the crystal, the chromophores must exhibit the same structural features (space groups, content of the asymmetric unit cell, intermolecular contacts). Requirement 3: additional macroscopic parameters, such as powder calibration, quality of crystals, refraction indexes, and phase-matching capabilities must be the same in all instances.

Requirement 1 is fulfilled, except for complex 7, for which the UV–vis transitions exhibit reduced intensity (reduction in β magnitude), while the presence of additional π -conjugation may significantly affect the β direction. With this respect, 7 can hardly be taken into account in the comparison of the SHG efficiencies. In addition, a molecule of water is present in the asymmetric unit cell of 7, leading to additional intermolecular contacts. Therefore, requirement 2 also is not fulfilled in the case of 7. By contrast, our investigation has provided a unique example of a set of molecules (2–6) with (i) the same molecular NLO response, (ii) the same chiral space group, and (iii) the same asymmetric unit cell content. The shortest intermolecular distances are roughly similar in the series (2.36–2.57 Å range). All of them involve the O3 atom and lead to very small hydrogen contacts. Furthermore,

(36) Kelvin, W. T. *Baltimore Lectures on Molecular Dynamics and the Wave Theory of Light*; C. J. Clay and Sons: London, 1904; pp 439 and 618.

(37) Mislow, K.; Bickart, P. *Isr. J. Chem.* **1976/77**, 15, 1.

(38) Buda, A. B.; Auf der Heyde, T.; Mislow, K. *Angew. Chem., Int. Ed. Engl.* **1992**, 31, 1, 989.

(39) Weinberg, N.; Mislow, K. *J. Math. Chem.* **1995**, 17, 35.

(40) (a) Zabrodsky, H.; Peleg, S.; Avnir, D. *J. Am. Chem. Soc.* **1992**, 114, 7843. (b) Zabrodsky, H.; Avnir, D. *J. Am. Chem. Soc.* **1995**, 117, 462.

(41) For example: Lipkowitz, K. B.; Schefzick, S.; Avnir, D. *J. Am. Chem. Soc.* **2001**, 123, 6710.

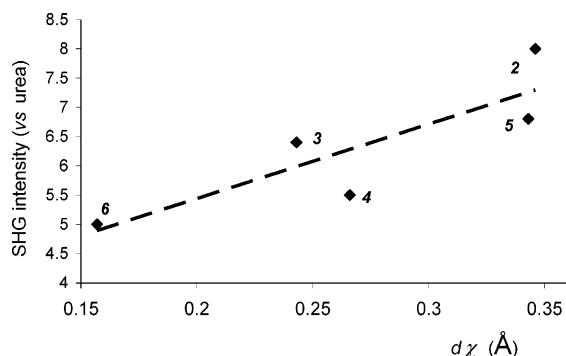


Figure 6. SHG intensities, expressed as a function of $d\chi$, for compounds 2, 3, 5, and 6, in which the same intermolecular interactions take place.

the chiral substituents are not involved in intermolecular interactions. Additionally, the asymmetric atom (C8) belongs to the rigid skeleton from which the charge transfer is originated. This latter observation suggests that the molecular orientation imposed by steric hindrances at the C8 level will necessarily have a direct counterpart in the orientation of the NLO moieties of the complex. Therefore, the β orientation should be correlated with the geometric features of the chiral substituents, at least to some extent. All together, these features lead to the assumption that requirement 2 is fulfilled in the 2–6 series.

The examination of requirement 3 reveals that it is based on several assumptions, which cannot be easily verified. Certainly, the powder calibration was carefully performed, and the starting materials were crystals of good quality obtained by slow evaporation. However, this does not guarantee that the crystal quality is strictly the same, in every sample. Furthermore, the statement that the refraction indexes are the same, because the molecules belong to the same family of tin complexes, is certainly valid in gas phase or solution but may become a crude assumption in the solid state. Finally, we have checked that the crystal size dependence of the SHG signals in the 50–80, 80–125, and 125–180 μm calibration range is modest (less than 30% in any case), leading to the assumption that the role of the phase-matching behavior is not dominant in the series. Nevertheless, and to minimize this effect, the samples used for the SHG comparison were those having the smallest calibration range (50–80 μm).²² Within these approximations, the SHG intensities are compared with the $d\chi$ parameter in Figure 6 for derivatives 2–6. The figure reveals a quite good correlation, which supports the anticipated idea that the more chiral molecules could be those providing the more SHG efficient solid, in a series of isostructural derivatives having the same β value.

In the past decade, NLO properties of various chiral molecules were reported with the observation that the more

chiral ones were exhibiting the larger SHG efficiencies.^{34,42} However, this is the first time that this trend is investigated in a series of five molecules. In the present case, the fact that the additional compound 7 provides the more chiral molecule, but finally the less efficient crystal, is certainly related to a different β magnitude and direction in this latter compound, together with a different asymmetric unit cell. Nevertheless, it points out the limitation of the methodology, which will certainly never be fully reliable at a large scale. Quantifying chirality by means of NLO measurements remains a challenge and must be restricted to few ideal situations in which molecules with strictly similar “push–pull” π -conjugated units and nonconjugated chiral substituents are perfectly isolated in the solid state within the same set of crystal symmetries.

Conclusion

The design of a large family of chiral push–pull organotin derivatives has been achieved in one step and has led to solid-state materials exhibiting sizable SHG efficiencies up to 8 times that of urea in second-harmonic generation, in addition with good transparencies ($\lambda_{\text{max}} < 400$ nm). A simple geometric parameter calculated from the X-ray structural data has been proposed as the molecular degree of chirality ($d\chi$) for these complexes. A correlation was observed between $d\chi$ and the specific rotation of the chromophores. Furthermore, an additional correlation was also observed between $d\chi$ and the solid-state SHG efficiencies of the derivatives, which possess the same molecular and solid-state electronic and structural features. This investigation provides a unique example of a possible quantification of molecular chirality by means of NLO measurements.

Acknowledgment. The authors thank CALMIP (Calcul intensif en Midi-Pyrénées, Toulouse–France) for computing facilities and acknowledge financial support from Consejo Nacional de Ciencia y Tecnología (CONACYT, México) and CNRS (France) (Project No. 15058). Thanks are given to Consejo Superior de la Investigación Científica in Spain for the Cambridge Crystallographic Data Base license. We also thank Q. Ma Luisa Rodríguez, QI Víctor González for NMR spectra, G. Cuéllar for mass spectra, and D. Castillo for IR spectra.

Supporting Information Available: IR, MS, optical rotation, elemental analyses, mp, and yields as well as the UV–vis spectrum for **1** (PDF). This material is available free of charge via the Internet at <http://pubs.acs.org>.

CM051589+

(42) For example: Balavoine, G. G. A.; Daran, J. C.; Iftime, G.; Lacroix, P. G.; Manoury, E. *Organometallics* **1999**, *18*, 21.